Technical Brief

Disease Modeling with 3D Cell-Based Assays Using a Novel Flowchip System and High-Content Imaging

SLAS Technology
1–12

DOI: 10.1177/2472630321000688
journals.sagepub.com/home/jla
SAGE

Evan F. Cromwell[1], Michelle Leung[1], Matthew Hammer[2], Anthony Thai[1], Rashmi Rajendra[1], and Oksana Sirenko[2]

Abstract

There is an increasing interest in using three-dimensional (3D) cell structures for modeling tumors, organs, and tissue to accelerate translational research. We describe here a novel automated organoid assay system (the Pu·MA System) combined with microfluidic-based flowchips that can facilitate 3D cell-based assays. The flowchip is composed of sample wells, which contain organoids, connected to additional multiple wells that can hold various assay reagents. Organoids are positioned in a protected chamber in sample wells, and fluids are exchanged from side reservoirs using pressure-driven flow. Media exchange, sample staining, wash steps, and other processes can be performed without disruption to or loss of 3D sample. The bottom of the sample chamber is thin, optically clear plastic compatible with high-content imaging (HCI). The whole system can be kept in an incubator, allowing long-term cellular assays to be performed. We present two examples of use of the system for biological research. In the first example, cytotoxicity effects of anticancer drugs were evaluated on HeLa and HepG2 spheroids using HCI and vascular endothelial growth factor expression. In the second application, the flowchip system was used for the functional evaluation of Ca^{2+} oscillations in neurospheroids. Neurospheres were incubated with neuroactive compounds, and neuronal activity was assessed using Ca^{2+}-sensitive dyes and fast kinetic fluorescence imaging. This novel assay system using microfluidics enables automation of 3D cell-based cultures that mimic in vivo conditions, performs multidosing protocols and multiple media exchanges, provides gentle handling of spheroids and organoids, and allows a wide range of assay detection modalities.

Keywords

microfluidics, high-content imaging, 3D cell-based models, organoids, toxicity

Introduction

Converting ideas for new therapeutics into improvements in human health can be difficult because the drug development journey is exhaustive, is costly, and fails far too often, driving a need for more advanced screening technologies to increase biological relevance and reduce costs associated with experimentation. An important trend is the increased use of spheroids, organoids, and other three-dimensional (3D) cell models for drug discovery and development.[1–3] Organoid models have been used for ex vivo studies of various cancers, neurological diseases, and more recently viral interactions with lungs, hearts, brains, gut, and other critical tissues.[4] Significant improvements have been made in the formation of complex organoid structures, including co-cultures exhibiting organ-like function,[5] patient-derived samples for disease modeling,[6] inflammation response from viral infections,[7] and mature protocols to make reproducible organoids.[8]

Microfluidics has gained popularity during the past 20 years for its demonstrated success in manipulating small volumes of fluid to control chemical, biological, and physical processes.[9] Advancements in microfluidics have allowed scientists to model complex cell-based assays, in which it is uniquely suited for recapitulating the in vivo microenvironment.[10,11] These novel 3D model systems, however, tend to show greater variability than two-dimensional (2D) assays and are less amenable to complex assay automation and

[1]Protein Fluidics, Burlingame, CA, USA
[2]Molecular Devices, San Jose, CA, USA

Received Feb 2, 2021, and in revised form Feb 2, 2021. Accepted for publication Feb 7, 2021.

Corresponding Author:
Evan F. Cromwell, Protein Fluidics, Inc., 875 Cowan Road, Suite B, Burlingame, CA 94010, USA.
Email: ecromwell@proteinfluidics.com

Figure 1. Schematic of the automated organoid assay workflow coupled with high-content three-dimensional (3D) imaging.

processing. For example, some common steps such as media exchange, compound additions, and staining are more difficult in 3D format because they may lead to loss or physical disruption of 3D microtissues. This means that critical biology can be perturbed during these steps, compromising the ability of researchers to truly recapitulate in vivo conditions. This represents a challenge, but also a huge opportunity for next-generation technology to automate and change workflows that lead to breakthroughs and improve human health.

Combining fluidics technologies with cell-based assays is an active area of investigation in both academic and industrial settings, and several devices are commercially available; a few are discussed here. In one example, a multichamber microfluidic device with flexible structures and a membrane between chambers is used to recapitulate lung function (Alveolus Lung-Chip, Emulate, Boston, MA). It uses pressure activation through channels to stretch microtissue to simulate the lung airway environment.[12] It has been used to model lung inflammation, intestinal diseases, as well as infectivity by viral-like particles.[13] In another device (OrganoPlate, Mimetas, Leiden, the Netherlands), human cells are co-cultured in the microchannels with perfusion.[14] Cells are directed through microfluidic channels to form complex tissue structures, such as blood vessels or intestinal walls.[15] These can be used to model angiogenesis, intestinal diseases, neuronal development, or cancer.[16] In a third example, spheroids or organoids are placed in individual wells connected by microfluidic example channels, providing flow between wells (Akura Flow, InSphero, Schlieren, Switzerland).[1,17] Assays with this device have been demonstrated with a variety of organ models, including liver and pancreatic islets, and the device can emulate complex organ interactions.

We describe here the Pu·MA System, a novel automated organoid assay system based on a proprietary microfluidic flowchip, which can be coupled with high-content imaging (HCI) and fast fluorescence kinetic readouts (**Fig. 1**). The flowchip is composed of sample wells, which contain organoids, connected to multiple wells that can hold various assay reagents (e.g., media, compounds, buffers, and staining solutions). The flowchips are loaded into a Pu·MA System that is placed inside an incubator, allowing long-term cellular assays to be performed. Preloaded assay protocols automatically perform all steps for organoid incubation, compound additions, staining, washing, and other assay steps. Once the assay processing is finished, the flowchips are removed for downstream analysis like HCI or supernatant sampling. The system has been used for applications in the areas of long-term toxicity, oncology therapeutics, single-organoid secretion, and metabolite sampling. We present two examples of use of the system for drug discovery and biological research.

Materials and Methods

Automated Flowchip Assay

The Pu·MA System comprises a benchtop instrument, which easily fits into a standard tissue culture incubator, containing a microprocessor-controlled pneumatic system, a touchscreen interface, and a plate-holding chamber. A key component of the automation system is the Pu·MA System flowchip (**Fig. 2**). The flowchips are designed with chambers and wells in a convenient multiwell plate format [SLAS/ANSI (Society for Laboratory Automation and Screening/American National Standards Institute) 384-well plate standard] that are connected by microfluidic channels. Each flowchip has eight assay lanes with 10 connected wells; a plate of four flowchips provides 32 tests. The microfluidic channels are nominally 50 µM in height and range from 50 µM to 200 µM in width. The channels

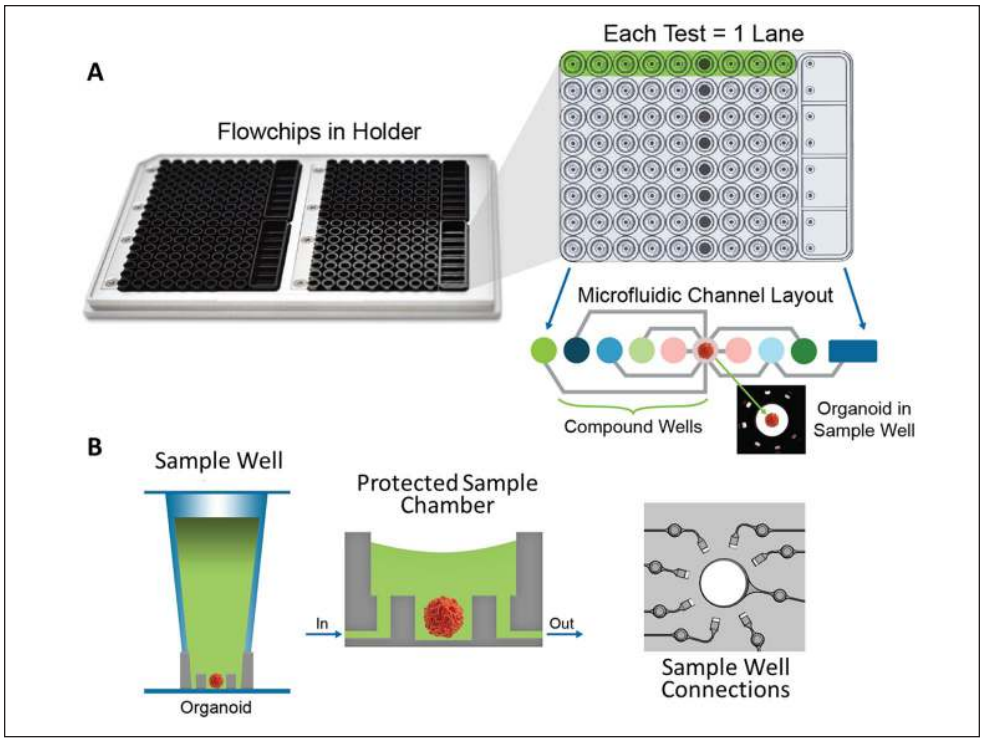

Figure 2. (**A**) Flowchip layout and microfluidic technology. Four flowchips (eight lanes each) are placed in a holder that locates all wells in a 384-multiwell plate format. The compound wells in each lane hold media, compounds, or additional assay reagents and are connected via microfluidic channels, allowing reagent exchanges between compound and sample wells. (**B**) Organoids are placed into the sample well and located in a protected chamber at the bottom of the well. This allows reagents to be directed in and out of the sample well without disturbing or drying out the microtissue. Eight wells are connected to the sample well: seven through side ports and one through a bottom port.

connecting to the sample well are designed to have equivalent resistances to balance fluid flow rates. Seven wells are connected to the sample well via side ports, allowing fluid exchange to occur without disturbing organoids in the protected chamber (**Fig. 2B**). One well is connected directly to the bottom of the protected chamber. This allows for the complete removal of fluid from the sample well if desired, as well as a path to remove trapped gas in the bottom of the well. The flowchips are made from black cyclic olefin copolymer (COC) with a thin, optically clear COC bottom suitable for multiple assay readouts, including high-resolution imaging. The flowchips are formed by injection molding and sealed with COC film by a solvent-bonding method. Use of injection molding provides high repeatability of the flowchip performance and fluid flow characteristics.

Microtissues, media, compounds, or other reagents are preloaded into the flowchip by pipetting, similarly as into a regular microplate. Reagents and spheroids can be loaded into the device manually or by using any automated 384-well-compatible liquid dispense system. Spheroids or organoids are positioned into a special protected chamber at the bottom of the sample well. After sample loading, the plate is placed into the Pu·MA System, and reagent exchanges are done automatically through the microfluidic channels. Importantly, there are no tubing connections between wells and the manifold, allowing flowchips to be easily placed into and removed from the device. Multiple reagent exchanges can be performed sequentially, enabling complex assay protocols and workflows to be run in an automated workflow with no manual processing. Typical assay protocols are preloaded into the system and can be selected with a touchscreen interface. Protocols can be modified according to the user's custom protocol.

The Pu·MA System can be placed in an incubator to run assays at 37 °C and 5% CO_2 (**Fig. 1**). The system architecture and use of pneumatics to move fluids provide gas exchange to the sample chambers. The underlying technology of the microfluidic device is valveless fluidic switching (VLFS).[18] Hydrophobic barriers (HPBs) at entrances and exits of the channels keep fluids in place until pneumatic pressure differentials are applied to move the fluids from well to well. The principles of hydrophobic burst valves have been previously described.[19] They are constructed by a combination of channel geometry and surface energy. The design balances a desire for a high burst valve pressure (e.g., a small channel opening) with a need to achieve robust and reproducible fluid flow. The channel entrances are nominally 50 μM in height, achieving a high cross section differential to the reservoir while minimizing the potential for clogging (e.g., cellular debris). COC is slightly hydrophobic with a contact angle of ~90°,[20] so to increase the HPB, the surfaces are coated with a proprietary material to increase the contact angle. An on-board microprocessor-based controller provides instructions to the pressure control system on how to manipulate fluids simultaneously for all 32 test lanes to perform complex assay protocols.

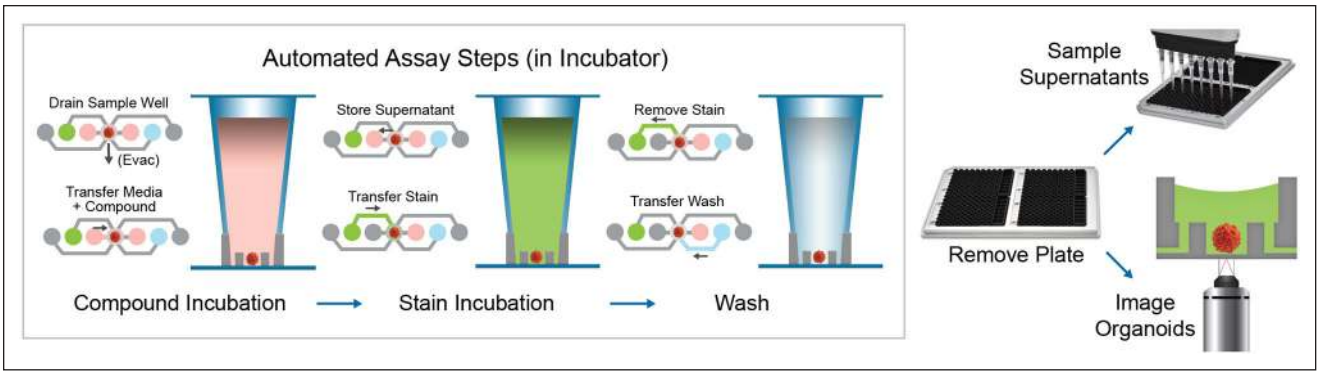

Figure 3. Fluid transfer steps presented for compound incubation, organoid staining, and stain removal by wash. Plates can be easily moved in and out of the system for downstream analysis. After a plate is removed from the Pu·MA System, supernatants can be removed for an enzyme-linked immunosorbent assay (ELISA) or other analysis. Microtissues can be imaged using an automated confocal imaging system or processed for other readouts.

The flowchip has been optimized to hold and manipulate 3D cell models such as organoids, spheroids, tumoroids, and microtissues. In this application, spheroids are formed externally and then placed into a sample well along with 20 µL of buffer or media. Other reagents used in an assay are dispensed into adjacent wells, where they can be exchanged one by one to perform the assay protocol (**Fig. 2**). A protected chamber with a volume of 0.8 µL is located at the bottom of the well, where the spheroid is located (**Fig. 2**). This allows imaging of the cells through the optically clear bottom of the flowchip. It also provides a region that safely holds the sample within the fluid during reagent exchange processes. This minimizes any perturbation to the cells during these processes and ensures that the spheroids do not dry out at any time. A flowchip holder locates all wells on the grid of a 384-multiwell plate format, making it compatible with most automated imaging systems and plate readers.

Cell Models

HeLa, HCT116, and HepG2 cell lines were obtained from ATCC (American Type Culture Collection; Manassas, VA) and maintained according to the manufacturer's recommendations. Appropriate media and supplements were obtained from Gibco (Thermo Fisher, Waltham, MA), as previously described.[3] For the concentration–response studies and phenotypic assay, cells were pre-plated into 96-well or 384-well, ultralow attachment, U-shaped black clear-bottomed plates (Corning 4520 and 3830, respectively; Corning, Corning, NY), at densities of 1000–4000 cells/well, in the appropriate media at 37 °C and 5% CO_2. Spheroids were formed during a 2–3-day period and then transferred into flowchips. A subset of experiments was done using magnetic particles to form or coat the spheroids (NanoShuttle, Greiner Bio-One, Austria) following published protocols.[21,22] The magnetized spheroids were directed to the bottom of the protected chamber and held in place by magnets located underneath the flowchips. Neurospheroids (microBrain 3D, StemoniX, Maple Grove, MN) were received from StemoniX and used after several days of additional culture according to their protocols.

Chemicals and Treatments

For compound screening, chemicals were prepared as 10–100 mM stock solutions in tissue culture–grade DMSO (Sigma-Aldrich, St. Louis, MO). The final concentration of DMSO in media was 0.1%. For spheroid toxicity, compounds (Sigma-Aldrich) were typically tested in duplicates in a six-point dilution series. Spheroids were transferred into flowchips and treated by performing an automated media exchange (**Fig. 3**). Cells were then exposed to the various concentrations of compounds for 48 h. For the calcium oscillation assay, neurospheroids were treated with compounds for 1 h.

Multiparametric Live Cell Toxicity Assay

The method for imaging and high-content analysis of 3D spheroids was previously described.[3] Briefly, following incubation with test compounds, spheroids were stained with a mixture of three dyes: 1 µM calcein AM, 3 µM ethidium homodimer-1 (EthD1), and 33 µM Hoechst 33342 (Life Technologies, Carlsbad, CA). Dyes were prepared in sterile phosphate buffered saline (PBS; Corning). In separate experiments, NucView 488 Green (1 µM) was used instead of calcein AM for assessment of cell apoptosis. Automated staining of the spheroids was performed for 2–3 h. In some experiments, dye solution was replaced with 1× PBS as a wash step at the end of the process (**Fig. 3**). Spheroid media after incubation were sampled from the

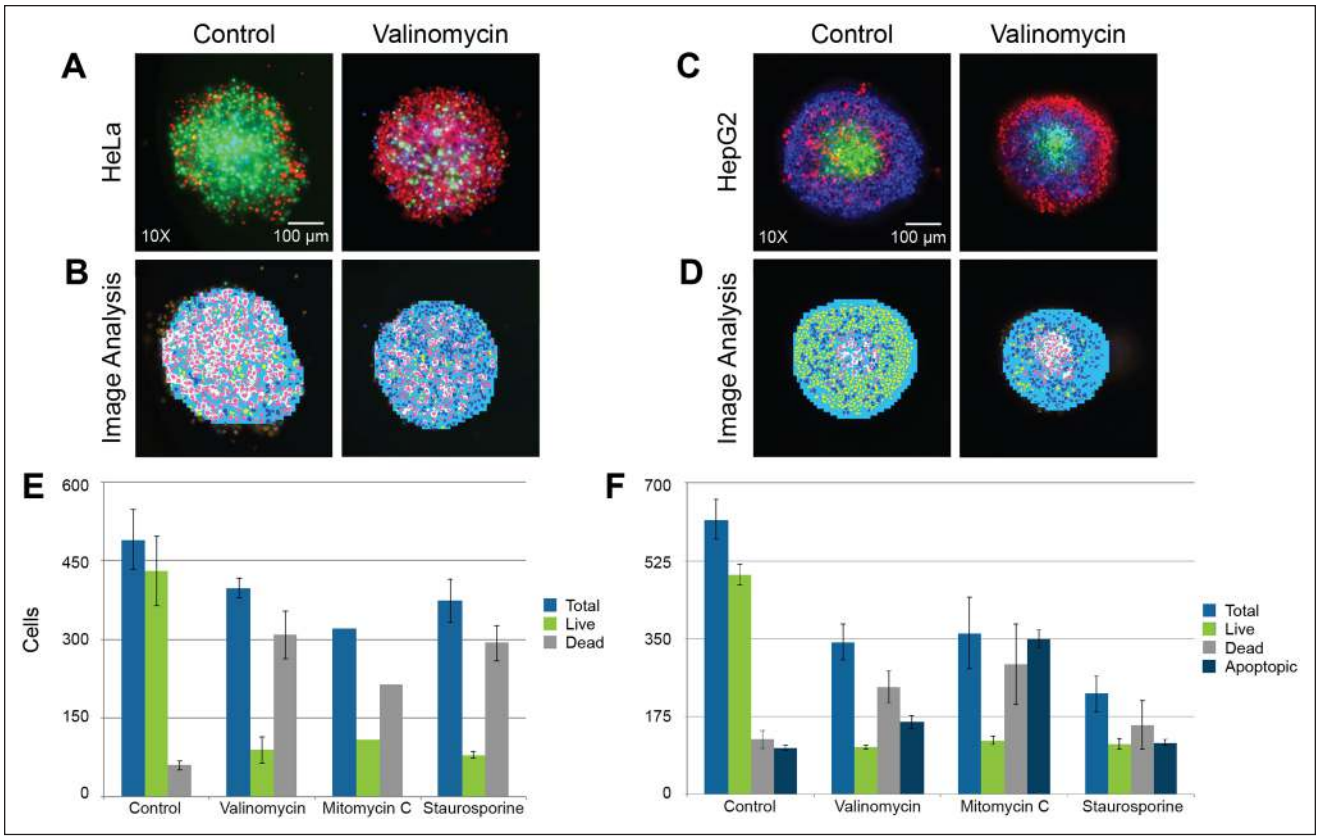

Figure 4. Image analysis of HeLa and HepG2 spheroids using confocal imaging. HeLa and HepG2 spheroids were incubated in the Pu·MA System with several anticancer compounds, as described in the Materials and Methods section. Spheroids were stained with a cocktail of several dyes and imaged using an ImageXpress Micro Confocal system. (**A,C**) Maximum projection images shown for untreated HeLa and HepG2 spheroids (control) and treated (valinomycin, 1 µM) HeLa and HepG2 spheroids. (**B,D**) Image analysis masks shown below the images. HeLa cells were stained with Hoechst nuclear dye (blue), calcein AM viability dye (green), and ethidium homodimer-1 (EthD1) dead cells dye (red). HeLa spheroids analysis shows spheroids (light blue), live cells' nuclei (red), live cells' cytoplasm (white), and dead cells' nuclei (dark blue). HepG2 cells were stained with Hoechst nuclear stain (blue), EthD1 dye (red), and NucView dye for apoptotic cells (green). HepG2 analysis shows spheroids (light blue), live cells' nuclei (yellow), dead cells' nuclei (dark blue), and apoptotic cells (red). (**E,F**) Bar graphs showing corresponding numbers of different cells in (**E**) HeLa and (**F**) HepG2 spheroids treated with 1 µM of indicated compounds.

flowchips for vascular endothelial growth factor (VEGF) analysis. Duplicate samples were combined, diluted 1:5.5, and run using a 96-well plate enzyme-linked immunosorbent assay (ELISA; Human VEGF DuoSet ELISA, R&D Systems, Minneapolis, MN) and measured on an absorbance plate reader. VEGF amount was quantified using standards and protocols provided in the ELISA kit.

High-Content Imaging

Images were acquired using a widefield or confocal automatic imaging system, ImageXpress Micro Confocal High-Content Imaging System (Molecular Devices, San Jose, CA), as previously described,[23] with a 10× Plan Fluor objective or 20× Plan Apo (**Fig. 4**). 4′,6-diamidino-2-phenylindole (DAPI), fluorescein isothiocyanate (FITC), and Texas Red filter sets were used for imaging. A stack of 7–15 images separated by 10–15 µm was acquired, starting at the well bottom and covering approximately the lower half of each spheroid. Typically, a Z-stack of images covered 100–200 µm for spheroids. Image analysis was performed either in 3D or by using the 2D Projection (maximum projection) images of confocal image stacks. Transmitted light images were used for cell culture monitoring or protocol optimization.

Image Analysis

Images were analyzed using the MetaXpress High-Content Image Acquisition and Analysis Software (Molecular Devices). The Count Nuclei and Cell Scoring application modules were used for nuclear count and live/dead assessment, respectively. A customized analysis for additional

multiparametric outputs was done using a protocol created in the MetaXpress Custom Module Editor (CME). The custom module analysis first identified the spheroid using Hoechst staining. Then, viable cells were identified by the presence of calcein AM or by the absence of EthD1 signal, and dead cells were identified by the presence of EthD1 signal. Apoptotic cells were defined using NucView stain. Output measurements included spheroid width, spheroid area, average intensity for calcein AM or EthD1, counts of all nuclei, and evaluation of average nuclear size and average intensities. In addition, calcein AM–positive cells were counted, and their area and intensity values were recorded. In addition to cell count, areas and intensities could be determined for live (EthD1-negative) and dead (EthD1-positive) cells. Transmitted light images could also be characterized by CME (not shown). EC_{50} values were determined using four-parameter curve fits from SoftMax Pro 6 Software (Molecular Devices).

Calcium Oscillation Assay

The intracellular Ca^{2+} oscillations in 3D neural cultures were assessed using the FLIPR Calcium 6 Kit (Molecular Devices), as described previously.[24] Calcium dye interacts with intracellular Ca^{2+}, and fluorescence intensity changes according to fluctuations in intracellular Ca^{2+} concentration. Kinetics of intracellular Ca^{2+} oscillations were determined by measuring fluorescence intensity at 515–575 nm following excitation at 470–495 nm for 10 min at a frequency of 3 Hz using the FLIPR Tetra High-Throughput Cellular Screening System (Molecular Devices). The exposure time per read was 0.4 s, the gain was 2000, and the excitation intensity was 30%. The instrument temperature was kept at a constant 37 °C. For acute exposure to compounds, cells were preloaded with Calcium 6 dye for 2 h prior to compound addition. Baseline for calcium oscillations without compounds was measured prior to compound addition. Then compounds were added, and effects on Ca^{2+} oscillations were measured after 60 min of exposure. Increased concentrations of compounds were added automatically to the same microtissues twice, and additional recordings were taken 30 min after each addition. For quantitative data evaluation, representative descriptors, such as peak count (per 10 min), average peak amplitude, average peak width (at 10% amplitude), average peak spacing (time between peaks), average peak rise time (from 10% to 90% amplitude), and average peak decay time (from 90% to 10% amplitude), were automatically derived using the ScreenWorks Peak Pro software package (version 4.2; Molecular Devices). Cell viability after 24 h of treatment was assessed using quantitative imaging of viable cells following staining with calcein AM and MitoTracker Orange CMTMRos, as described below. Individual compounds were tested in 6–7 concentrations, typically in triplicate.

Results

Automated Culture of 3D Microtissues Using the Pu·MA System

The processes of culture, treatment, staining, and manipulation with spheroids and organoids are typically labor-intensive because caution is practiced heavily to decrease the risk of disrupting or destroying the samples. 3D culture protocols are typically more complex, requiring additional optimization, and limiting wide adoption of the techniques due to higher complexity. The Pu·MA System, described in detail above, is designed to provide automated cell culture and processing of 3D cell model samples such as spheroids and organoids. The system operates in an incubator using a pneumatic pumping system to automatically move liquids in flowchips holding 3D cell samples, culture media, and assay reagents. Performing all assay steps in an incubator enables environmental control for assays and toxicity evaluation. The flowchips are composed of a sample chamber and reagent wells in a multiwell plate format that are connected by microfluidic channels. Spheroids or organoids are positioned within the special protected chamber at the bottom of the sample well. Preloaded protocols execute fluid movements simultaneously for all 32 test lanes to perform complex assay protocols.

The goal of the present work was to develop and optimize methods using the pneumatic control system and flowchips for automated 3D cell model culture and treatment of 3D microtissues. Use of specially designed organoid sample chambers and microfluidic connections to reagent wells alleviates workflow challenges for 3D culture. The 384-multiwell plate format integrates easily with existing liquid handlers and other downstream processing systems for a seamless workflow. Furthermore, because the flowchips have standard plate dimensions and are not connected to external tubes, they are compatible with various imaging instruments and plate readers, and can be taken out of the device to be imaged by the ImageXpress Micro Confocal system for various cell markers.

As shown in **Figure 3**, the first step after loading flowchips in the Pu·MA System is to exchange media with fresh media or media + compound treatment. The microfluidic configuration allows exchange of approximately 95% of the media without drying the cells or disrupting the spheroids. Spheroids were then incubated for a predetermined amount of time within the incubator. Gas exchange between the incubator and media is accomplished by pulsing air in and out of the manifold. The temperature at the flowchips is equilibrated with the incubator. A 48-h cell culture protocol was performed automatically, which included two media exchanges with re-addition of compounds, then addition of viability dyes, and a final wash of spheroids from staining reagents. At that point, spheroids were ready for imaging. In

addition, following incubation, the media were removed from adjacent wells and sampled for downstream analysis by ELISA. For HeLa spheroids, the compound incubation period was 22 h, followed by a 2-h staining incubation. For HepG2 spheroids, the compound incubation was 44 h again, followed by a 2-h staining. Spheroids remained in the protected chamber during the course of the assay protocol. The 3D samples were then imaged, as described below.

Automated Assessment of Compound Responses Using 3D Spheroid Cultures

We automated a 3D assay protocol with cancer spheroids using the Pu·Ma System. Spheroids were formed with HeLa or HepG2 cancer cells, and the effects of selected cytotoxic drugs were evaluated by imaging and VEGF expression. The black walls of the flowchip wells and the thin, optically clear bottom of the flowchip make the device compatible with high-resolution fluorescence imaging or a plate reader device (e.g., fluorescence or luminescence detection). During the processing, HeLa spheroids were stained with a mixture of three dyes: Hoechst 33342 (nuclear stain), calcein AM (viability dye), and EthD1 for marking dead cells (as described in the Materials and Methods section). For staining of the HepG2 spheroids, NucView 488 Green was substituted for calcein AM to detect apoptotic cells.

Flowchips were taken out of the device and imaged by the ImageXpress Micro Confocal system for various cell viability markers. Confocal imaging provided 3D cellular resolution of spheroid structures to observe the size and integrity of spheroids, as well as the number of total, viable, and affected cells. Detailed image analysis allowed determination of the impact of compound treatment by the characterization of nuclei, mitochondria, viability, and apoptotic markers. Spheroids were imaged at 10× or 20× magnification, and a Z-stack of images was taken using an 8–15 μM interval. Importantly, at 10× magnification, the bottom of a sample well was captured in one single site, allowing easy analysis of spheroid morphology. Images of treated and untreated spheroids are shown in **Figure 4**. There were observed marked changes in the spheroid phenotypes: decrease of live cell staining (calcein AM–positive) and increase in the number of dead cells (EthD1-positive) with all compounds.

Image analysis was done on maximum projection images for detection of the numbers and percentages of total cells (count nuclei), live cells (EthD1-negative or calcein AM–positive cells), dead cells (EthD1-positive or calcein AM–negative), and apoptotic cells (NucView-positive). Custom module analysis was used (MetaXpress software, Molecular Devices) for finding spheroids, then defining cells with different phenotypes within spheroids (**Fig. 4D and 4E**). The bar graphs in **Figure 4** show the numbers of total cells, live cells, dead cells, and apoptotic cells in the control and treated samples. Three cytotoxic compounds—staurosporine, mitomycin C, and valinomycin—demonstrated expected effects on cell viability in both cell lines. **Figure 5** shows concentration-dependent changes in spheroid phenotypes with increasing concentrations of staurosporine. Phenotypic changes were quantitated by counting the numbers of cells that were positive or negative for different markers, and by measuring the average intensities of stains, cell areas, or spheroid areas. Concentration dependencies of the percentages of live and dead cells are shown in **Figure 5**. EC_{50} values for different compound effects were calculated from using four-parametric curve fits and are shown in **Table 1**.

Conditioned media were removed from the flowchips after the compound incubation period. Duplicate samples were combined together and diluted in assay buffer by 1:5.5. This provided sufficient volume to run a 96-well plate ELISA. No VEGF was detected in samples from the HeLa spheroids. Concentration dependence of VEGF from HepG2 spheroids treated with staurosporine is shown in **Figure 5E**. A clear decrease in VEGF is observed, consistent with increased spheroid toxicity.

Functional Evaluation of Calcium Oscillations in Neurospheroids

In a second application, the flowchip system was used for the functional evaluation of calcium oscillations in induced pluripotent stem cell (iPSC)-derived neurospheroids on treatment with neuroactive compounds.[25] The microBrain 3D neural cell microtissues are composed of two neural cell types: cortical neurons and astrocytes. They demonstrate spontaneous activations that can be observed by monitoring oscillations of calcium sensor dye. Neurospheroids generate functional activity that was assessed via Ca^2+ oscillations using fast kinetic fluorescence imaging. We have previously described the method, compound responses. and toxicity assessment of neurospheroids using recording and analysis of calcium oscillations patterns.[24]

In the present protocol, we have used the flowchip system for sequential additions of compounds and for determining a concentration response by recording measurements from the same microtissue. Neurospheroids were placed into a flowchip and incubated with various known neuromodulator compounds. The Pu·MA System was used for single or multiple additions of compounds, from low to high concentrations, to the neurospheroids. We have observed changes of calcium oscillation patterns from control and neurospheroids treated with various neuromodulators, including inhibitors and activators of neural activity, and tested several neurotoxic compounds. **Figure 6** shows the effects of gabapentin,[26] an agonist of inhibitory neurons, and azimilide,[27] an antiarrhythmic drug and hERG channel blocker, on

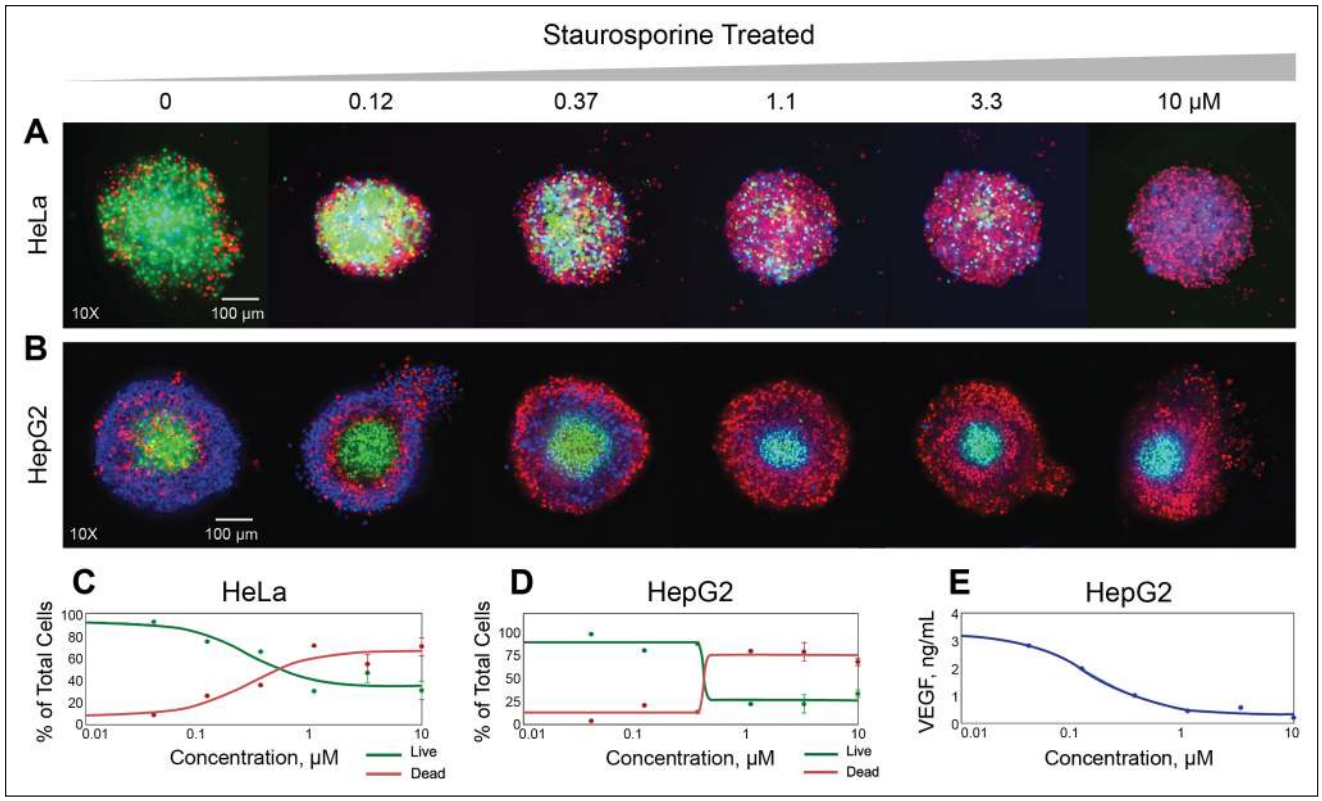

Figure 5. Quantitative assessment of the effect of staurosporine on spheroid morphology and viability by high-content imaging. HeLa and HepG2 spheroids were incubated in the Pu·MA System with several anticancer compounds, as described in the Materials and Methods section. Three-dimensional (3D) spheroids were stained with combinations of several dyes and imaged using an ImageXpress Micro Confocal system. Maximum projection images are shown for (**A**) HeLa and (**B**) HepG2 control spheroids and spheroids treated with indicated increasing concentrations of staurosporine. HeLa cells were stained with Hoechst nuclear dye (blue), calcein AM viability dye (green), and ethidium homodimer-1 (EthD1) dead cells dye (red). HepG2 cells were stained with Hoechst nuclear stain (blue) and EthD1 dye (red), with NucView dye for apoptotic cells (green). (**C,D**) Concentration-dependent plots shown for percentages of live cells and dead cells quantitated in the images of spheroids for different concentrations of staurosporine. (**E**) Concentration of vascular endothelial growth factor (VEGF) measured in supernatants from HepG2 spheroids as a function of staurosporine concentration. Supernatants from two spheroids were combined and analyzed by enzyme-linked immunosorbent assay (ELISA) for each measurement.

Table 1. EC_{50} Values Defined from the Concentration Dependencies of the Percentages of Live Cells and Dead Cells Counted by High-Content Imaging.

	HeLa EC_{50} (µM)		HepG2 EC_{50} (µM)	
	% Live Cells	% Dead Cells	% Live Cells	% Dead Cells
Staurosporine	0.29	0.29	0.41	0.42
Valinomycin	0.054	0.054	0.12	0.13
Mitomycin C	15.1	15	5.05	5.04

Note: EC_{50} values were determined by four-parametric curve fits.

calcium oscillations. The flowchips were analyzed on the FLIPR Tetra system after neurospheroid loading [**Fig. 6C**, first (control)] and then after each compound exchange (**Fig. 6C**, second and third). Neurospheroids were equilibrated with Calcium 6 dye for 60 min after loading into the flowchips, and then they were incubated for 30 min with each of the compound concentrations. Kinetic fluorescence patterns were recorded directly in the flowchip plates and demonstrated modulation in neural network activity of the spheroids.

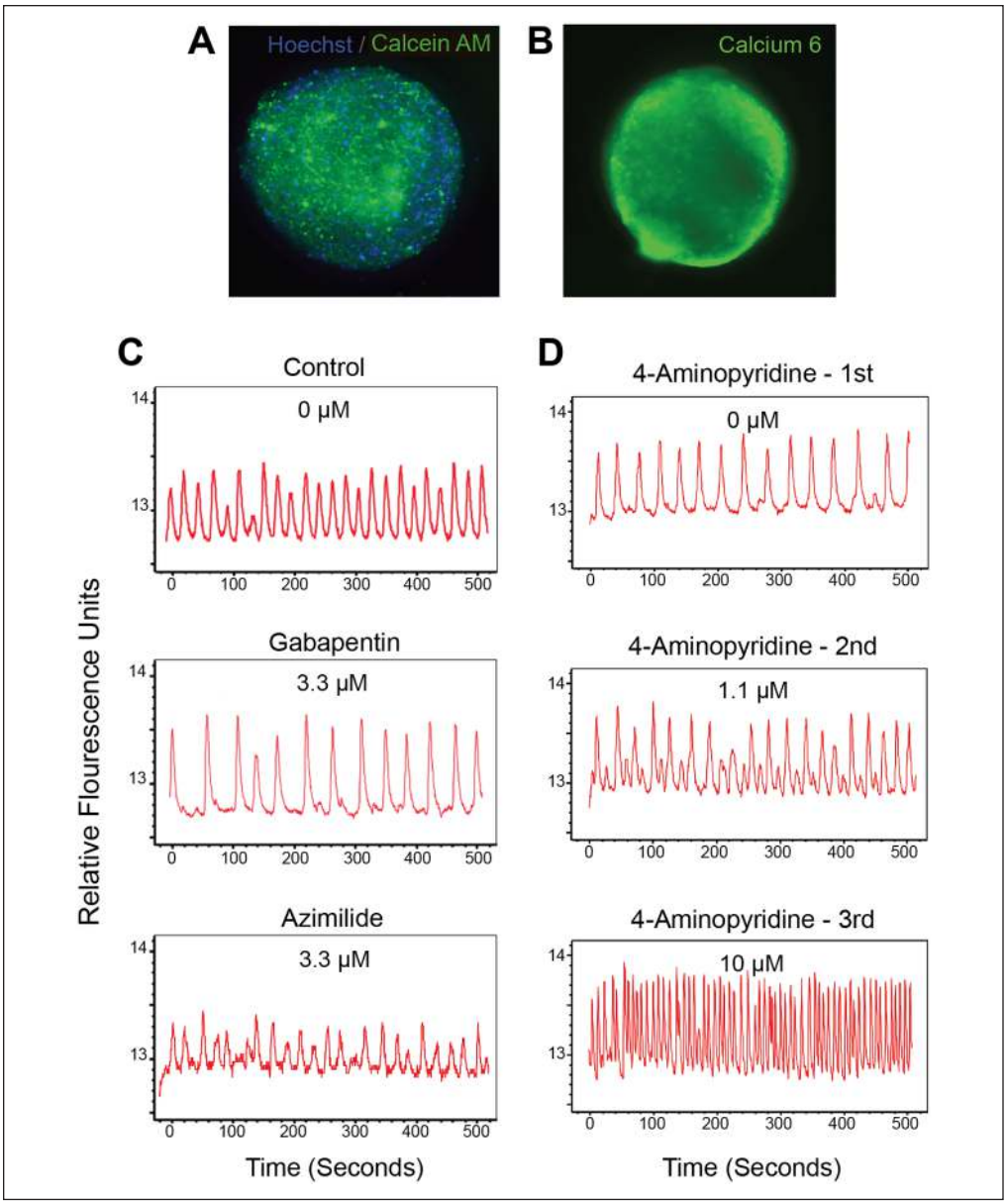

Figure 6. High-content imaging and recordings of $Ca^{2}+$ oscillations in neurospheroids. (**A**) Two-dimensional (2D) projection image of a neurospheroid stained with Hoechst (blue), calcein AM (green), and ethidium homodimer-1 (EthD1; red), as described in **Figure 4**. (**B**) Image of neurospheroid stained with Calcium 6 dye. (**C,D**) Kinetic fluorescent recording of calcium oscillations measured by the FLIPR Tetra system. Recorded patterns were analyzed, and peaks counted by Peak Pro 2 software. Neurospheroids were stained with Calcium 6 dye and treated for 30 min with indicated compounds using the Pu·MA system, as described in the Materials and Methods section. (**D**) Concentration response of a single neurospheroid to 4-aminopyridine (4-AP). The first measurement was with media only, the second with 1.1 µM 4-AP after 30 min of incubation, and the third with 10 µM 4-AP after an additional 30 min of incubation.

Notably, while it is challenging to sequentially add and remove different solutions when working with spheroids or organoids, the automated microfluidics process allowed precise exchange of media and compound concentrations without disturbing microtissues, and it minimized systemic errors caused by incomplete exchange of compound concentrations. It also allowed for addition of different compounds to the same microtissue, washing off compounds, and observing changes in responses and dose responses in the same single spheroid. We also were able to automatically add, wash, or exchange different compounds into the same sample, allowing us to evaluate concentration responses of compound effects (**Fig. 6C**). In this example, 4-aminopyridine,[28] a potassium channel (Kv1) blocker and neurogenic agent, was added subsequently at two different concentrations (1.1 µM and 11 µM). Observed changes in the calcium oscillation activity were consistent with the expected mechanism of action of the compounds. Finally, neurospheroids were washed of the calcium sensor and stained with viability dyes, which allowed assessment of cell viability by HCI (**Fig. 6A**). None of the compounds tested in this study were observed to cause cell death in the neurospheroids within the time of the experiment, which is important information when evaluating functional effects.

Discussion

Various screening systems have been implemented to eliminate repetitive manual labor and accelerate the lead generation process.[29] The novel automated 3D organoid assay

system described here, the Pu·MA System, provides a way to automate complex assay workflows using special microfluidic flowchips. This system provides hands-free functionality that enables automatic 3D cell culture and sample processing. The system has an open platform design. Multiple assay process steps are enabled by having a spheroid or organoid sample connected to multiple wells that can hold different assay reagents. The different solutions can then be transferred to the samples sequentially using pneumatic pressure to allow multiple processing steps, such as media exchange, compound additions, sample staining with fluorescent dyes, washing, fixing, removal of media, and lysis if required. In contrast to traditional "organ-on-chip" devices, flowchips used with this system can be easily taken in and out from the device for reading on various instruments, or for additional manipulations or processing steps (e.g., freezing, DNA and RNA analysis, and metabolic profiling). As we demonstrated above, the plate holder and assay format are fully compatible with other instruments, including automated high-content imagers or kinetic fluorescence readers. Importantly, conditioned media or supernatant samples can be collected during the process and be analyzed by downstream processes such as ELISA, metabolomic profiling, and other assays. In addition, cells in the sample chamber can be analyzed for adenosine triphosphate (ATP) activity by introduction of appropriate reagents (e.g., CellTiter Glo 3D Viability Assay, Promega, Madison, WI), followed by luminescence measurement on a conventional plate reader.

This automated technology enables researchers to enhance the complexity and sophistication of experiments that can be performed on a microfluidic chip. A variety of automated steps can be performed, which can help avoid experimental errors or sample mix-up, and increase the consistency of the experiments. Multiple protocols can be used for various workflows, or protocols can be modified according to experimental needs. In addition, the experimental quality and convenience can be increased, since the flowchip provides gentle and more precise media exchange, including complete media drain or exchange, which is hardly achievable by using manual or automated pipetting steps (spheroids or organoids could be easily lost or destroyed during pipetting steps).

Small-Sample-Volume Benefits

Another benefit of the workflow is the low volume when performing assays, which can be very important to scientists dealing with limited samples of low-abundant analytes. The small size of the reservoirs and individual fluidic circuit components in the microfluidic device provides an arsenal of experimental advantages, which makes such solutions desirable. For example, small components enable researchers to perform experiments that are not possible or practical to execute with more traditional methods. Increased sensitivity can be obtained when cells in the 3D models secrete into a smaller volume, providing higher analyte concentrations. When analyzing the biological measurement of fluidic components at the cellular scale, microfluidic channels provide exceptional liquid-handling capabilities, allowing manipulation of single cells and even single molecules in vitro.[30] The automated microfluidic solution combined with high-content 3D imaging significantly help researchers save time on tedious manual labor and materials, and fundamentally lead to higher-precision measurements.

Future Directions

The limitations of the system at present are related to 32 samples per run, which is a trade-off for the convenience of containing multiple solutions within the same plate. Therefore, the system is most useful for relatively small- or medium-scale experiments. An alternative future design of the flowchip may include a version that would increase the number of test samples, while providing more limitations for the numbers of different reagents that could be included in the same process. Another limitation common to microfluidic systems is the possibility of clogging the channel, for example when tissues are dispersed by compound treatment. Pneumatic pressure–driven flow instead of tubing with pumps, however, has a lot of advantages in reliability, flexibility, and reduction of bubbles in the process. The current tested occurrence of clogging channels is estimated as $<1\%$ of the samples.

We demonstrated here use of the system for testing the cytotoxicity of various compounds and for sequential treatments of cells measuring functional responses. Other applications for the Pu·MA System include the use of patient-derived tissues and organoids for sensitivity/drug testing in fields such as cancer, inflammation studies, and metabolism research, with the goal of personalizing patient treatment. This system is especially beneficial to scientists using limited samples of starting material, like patient-derived samples or in patient-derived organoid research, translational research, preclinical studies, or patient response to specific drugs.

Conclusion

Technology, including the automated sample processing and precise control of fluids in an assay, has made microfluidics an attractive application to replace traditional experimental approaches.[1,30] Combining microfluidic systems to perform assays with 3D cell-based structures with automated confocal imaging and other advanced instruments offers a powerful tool to researchers looking to increase assay complexity, improve the efficiency of their phenotypic assays, and obtain the highest-value biological data from their research.

Acknowledgments

The authors would like to thank StemoniX for providing microBrain 3D neurospheres, and Carol Crittenden for assistance with FLIPR Tetra system experiments and data analysis.

Declaration of Conflicting Interests

The authors declared the following potential conflicts of interest with respect to the research, authorship, and/or publication of this article: The authors EFC, ML, AT, and RR are employed by Protein Fluidics, which manufactures the Pu·MA System. The authors OS and MH are employed by Molecular Devices, which manufactures the ImageXpress Micro Confocal and FLIPR Tetra systems.

Funding

The authors received no financial support for the research, authorship, and/or publication of this article.

References

1. Gupta, N.; Liu, J. R.; Patel, B.; et al. Microfluidics-Based 3D Cell Culture Models: Utility in Novel Drug Discovery and Delivery Research. *Bioeng. Transl. Med*. **2016**, *1*, 63–81.
2. Kochanek, S. J.; Close, D. A.; Johnston, P. A. High Content Screening Characterization of Head and Neck Squamous Cell Carcinoma Multicellular Tumor Spheroid Cultures Generated in 384-Well Ultra-Low Attachment Plates to Screen for Better Cancer Drug Leads. *Assay Drug Dev. Technol*. **2019**, *17*, 17–36.
3. Sirenko, O.; Mitlo, T.; Hesley, J.; et al. High-Content Assays for Characterizing the Viability and Morphology of 3D Cancer Spheroid Cultures. *Assay Drug Dev. Technol*. **2015**, *13*, 402–414.
4. Schutgens, F.; Clevers, H. Human Organoids: Tools for Understanding Biology and Treating Diseases. *Annu. Rev. Pathol. Mech. Dis*. **2020**, *15*, 211–234.
5. March, S.; Ramanan, V.; Trehan, K.; et al. Micropatterned Coculture of Primary Human Hepatocytes and Supportive Cells for the Study of Hepatotropic Pathogens. *Nat. Protoc*. **2015**, *10*, 2027–2053.
6. Strong, A. L.; Ohlstein, J. F.; Biagas, B. A.; et al. Leptin Produced by Obese Adipose Stromal/Stem Cells Enhances Proliferation and Metastasis of Estrogen Receptor Positive Breast Cancers. *Breast Cancer Res*. **2015**, *17*, 112.
7. Nawroth, J. C.; Lucchesi, C.; Cheng, D.; et al. A Micro-Engineered Airway Lung-Chip Models Key Features of Viral-Induced Exacerbation of Asthma. *Am. J. Respir. Cell Mol. Biol*. **2020**. doi:10.1165/rcmb.2020-0010MA.
8. Mohamed, N. V.; Larroquette, F.; Beitel, L. K.; et al. One Step into the Future: New iPSC Tools to Advance Research in Parkinson's Disease and Neurological Disorders. *J. Parkinsons Dis*. **2019**, *9*, 265–281.
9. Plevniak, K.; He, M. Microfluidic Technology: The Next Generation Drug Discovery Tool. *Drug Target Review*, September 21, 2015. https://www.drugtargetreview.com/article/6353/microfluidic-technology-the-next-generation-drug-discovery-tool/.
10. Junaid, A.; Mashaghi, A.; Hankemeier, T.; et al. An End-User Perspective on Organ-on-a-Chip: Assays and Usability Aspects. *Curr. Opin. Biomed. Eng*. **2017**, *1*, 15–22.
11. Ewart, L.; Dehne, E. M.; Fabre, K.; et al. Application of Microphysiological Systems to Enhance Safety Assessment in Drug Discovery. *Annu. Rev. Pharmacol. Toxicol*. **2018**, *58*, 65–82.
12. Benam, K. H.; Villenave, R.; Lucchesi, C.; et al. Small Airway-on-a-Chip Enables Analysis of Human Lung Inflammation and Drug Responses In Vitro. *Nat. Methods* **2016**, *13*, 151–157.
13. Park, S. E.; Georgescu, A.; Huh, D. Organoids-on-a-Chip. *Science* **2019**, *364*, 960–965.
14. Trietsch, S. J.; Israels, G. D.; Joore, J.; et al. Microfluidic Titer Plate for Stratified 3D Cell Culture. *Lab Chip* **2013**, *13*, 3548–3554.
15. Vormann, M. K.; Gijzen, L.; Hutter, S.; et al. Nephrotoxicity and Kidney Transport Assessment on 3D Perfused Proximal Tubules. *AAPS J*. **2018**, *20*, 90.
16. Bircsak, K. M.; DeBiasio, R.; Miedel, M.; et al. A 3D Microfluidic Liver Model for High Throughput Compound Toxicity Screening in the OrganoPlate(R). *Toxicology* **2021**, *450*, 152667.
17. Lohasz, C.; Rousset, N.; Renggli, K.; et al. Scalable Microfluidic Platform for Flexible Configuration of and Experiments with Microtissue Multiorgan Models. *SLAS Technol*. **2019**, *24*, 79–95.
18. Jiao, H.; Jensen, E. C.; Mehrabani, H.; et al. Reconfigurable Microfluidic Systems: Homogeneous Assays. U.S. Patent US9956558B2, **2018**.
19. Cho, H.; Kim, H. Y.; Kang, J. Y.; et al. How the Capillary Burst Microvalve Works. *J. Colloid, Interface Sci*, **2007**, *306*, 379–385.
20. Wang, B.; Wang, X.; Zheng, H.; et al. Surface Wettability Modification of Cyclic Olefin Polymer by Direct Femtosecond Laser Irradiation. *Nanomaterials (Basel)* **2015**, *5*, 1442–1453.
21. Haisler, W. L.; Timm, D. M.; Gage, J. A.; et al. Three-Dimensional Cell Culturing by Magnetic Levitation. *Nat. Protoc*. **2013**, *8*, 1940–1949.
22. Hou, S.; Tiriac, H.; Sridharan, B. P.; et al. Advanced Development of Primary Pancreatic Organoid Tumor Models for High-Throughput Phenotypic Drug Screening. *SLAS Discov*. **2018**, *23*, 574–584.
23. Grimm, F. A.; Iwata, Y.; Sirenko, O.; et al. High-Content Assay Multiplexing for Toxicity Screening in Induced Pluripotent Stem Cell-Derived Cardiomyocytes and Hepatocytes. *Assay Drug Dev. Technol*. **2015**, *13*, 529–546.
24. Sirenko, O.; Parham, F.; Dea, S.; et al. Functional and Mechanistic Neurotoxicity Profiling Using Human iPSC-Derived Neural 3D Cultures. *Toxicol. Sci*. **2019**, *167*, 58–76.
25. Sirenko, O.; Vargas-Hurlston, S.; Chandy, G.; et al. Functional Evaluation of Neurotoxic Compounds Using Human iPSC-Derived Neuronal 3D Cultures. *J. Pharmacol. Toxicol. Methods* **2019**, *99*, 106595.
26. Calandre, E. P.; Rico-Villademoros, F.; Slim, M. Alpha2delta Ligands, Gabapentin, Pregabalin and Mirogabalin: A Review

of Their Clinical Pharmacology and Therapeutic Use. *Expert Rev. Neurother*. **2016**, *16*, 1263–1277.
27. Busch, A. E.; Eigenberger, B.; Jurkiewicz, N. K.; et al. Blockade of HERG Channels by the Class III Antiarrhythmic Azimilide: Mode of Action. *Br. J. Pharmacol*. **1998**, *123*, 23–30.
28. Wu, Z. Z.; Li, D. P.; Chen, S. R.; et al. Aminopyridines Potentiate Synaptic and Neuromuscular Transmission by Targeting the Voltage-Activated Calcium Channel Beta Subunit. *J. Biol. Chem*. **2009**, *284*, 36453–36461.
29. Schneider, G. Automating Drug Discovery. *Nat. Rev. Drug Discov*. **2018**, *17*, 97–113.
30. Streets, A. M.; Huang, Y. Chip in a Lab: Microfluidics for Next Generation Life Science Research. *Biomicrofluidics* **2013**, *7*, 11302.